Check for updates

Received: 25 May 2021 | Accepted: 13 November 2021

DOI: 10.1111/1365-2435.13983

Functional Ecology | BRITISH ECOLOGICAL SOCIETY

RESEARCH ARTICLE

Power law scaling relationships link canopy structural complexity and height across forest types

Jeff W. Atkins[1,2] | Jonathan A. Walter[3,4] | Atticus E. L. Stovall[5,6] | Robert T. Fahey[7] | Christopher M. Gough[2]

[1]USDA Forest Service, Southern Research Station, New Ellenton, SC, USA; [2]Department of Biology, Virginia Commonwealth University, Richmond, VA, USA; [3]Department of Environmental Sciences, University of Virginia, Charlottesville, VA, USA; [4]Environmental Research Alliance, Charlottesville, VA, USA; [5]Biospheric Sciences Laboratory, NASA Goddard Space Flight Center, Greenbelt, MD, USA; [6]Department of Geographical Sciences, University of Maryland, College Park, MD, USA and [7]Department of Natural Resources and the Environment & Center for Environmental Sciences and Engineering, University of Connecticut, Storrs, CT, USA

Correspondence
Jeff W. Atkins
Email: jeffrey.atkins@usda.gov

Handling Editor: Emma Sayer

Abstract

1. Forest canopy structural complexity (CSC), an emergent ecosystem property, plays a critical role in controlling ecosystem productivity, resource acquisition and resource use-efficiency; yet is poorly characterized across broad geographic scales and is difficult to upscale from the plot to the landscape.
2. Here, we show that the relationship between canopy height and CSC can be explained using power laws by analysing lidar-derived CSC data from 17 temperate forest sites spanning over 17 degrees of latitude. Across three plant functional types (deciduous broadleaf, evergreen needleleaf and mixed forests), CSC increases as an approximate power law of forest height. In evergreen needleleaf forests, increases in canopy height do not result in increases in complexity to the same magnitude as in other forest types.
3. We attribute differences in the slope of height:complexity relationships among forest types to: (a) the limited diversity of crown architectures among evergreen conifer trees relative to broadleaf species; (b) differences in how vertical forest layering develops with height; and (c) competitive exclusion by needleleaf species. We show support for these potential mechanisms with an analysis of 4,324 individual trees from across 18 National Ecological Observatory Network sites showing that crown geometry-to-tree height relationships differ consistently between broadleaf and needleleaf species.
4. Power law relationships between forest height and CSC have broad implications for modelling, scaling and mapping forest structural attributes. Our results suggest that forest research and management should consider the nonlinearity in scaling between forest height and CSC and that the nature of these relationships may differ by forest type.

KEYWORDS
canopy structural complexity, forest complexity, forest structure, plant functional type, power law, scaling

© 2021 British Ecological Society. This article has been contributed to by US Government employees and their work is in the public domain in the USA.

1 | INTRODUCTION

Canopy structural complexity (CSC) is an emergent property of forests that integrates ecological characteristics across scales of individuals, species, communities and ecosystems (Aber et al., 1982; Ellsworth & Reich, 1993; Fahey et al., 2019; Fotis et al., 2018; Hardiman et al., 2013; Ishii et al., 2004; Parker et al., 1989). Canopy structural complexity arises from the arrangement of canopy photosynthetic and non-photosynthetic elements (Fotis & Curtis, 2017); however, the degree of complexity is bounded by forest height (Gough et al., 2020; West et al., 2009). Within the volume of the canopy, the structural configurations that manifest are a product of both abiotic and biotic controls including: species composition (Gough et al., 2020), tree architecture (Saarinen et al., 2021; Schraik et al., 2021), edaphic factors (Hulshof & Spasojevic, 2020), resource availability (Ehbrecht et al., 2021), competition, climate (Ehbrecht et al., 2021; Ishii & Asano, 2010) and physiography (Fahey et al., 2019). Canopy structural complexity is also strongly linked with ecosystem functioning including resource acquisition (Atkins, Fahey, et al., 2018), use-efficiency, productivity (Hardiman et al., 2013), microclimate regulation (Frenne et al., 2019) and habitat provisioning (Davies et al., 2017). A mathematically universal representation of these phenomena would provide a seamless connection across scales of organization, allowing the inference of complexity—a difficult to measure structural attribute—from canopy height—a relatively straightforward to measure structural attribute.

We propose that the relationship between canopy height and CSC can be described by a power law relationship, implying a scale invariant, universal relationship. There are numerous examples of power law relationships in ecology and environmental science (Seekell et al., 2013; Walter et al., 2020; West et al., 1997), and in forested ecosystems, power law relationships have been found among tree height–diameter relationships (i.e. allometric scaling; Duncanson et al., 2015; West et al., 1999), tree size distributions (Enquist et al., 2009; Farrior et al., 2016), live to dead basal area (Ferguson & Archibald, 2002), patterns of forest fragmentation (Taubert et al., 2018) and disturbance frequency (Kellner et al., 2011). One particular type of power law relationship, known in ecology as Taylor's law (Taylor, 1961), relates the variance of groups of samples to their means via a power law relationship. Taylor's law has been found to hold in a wide variety of empirical phenomena (Lagrue et al., 2015; Tippett & Cohen, 2016; Xu et al., 2015; Zhao et al., 2019) and is closely related to our forest canopy height:complexity scaling problem because many CSC metrics are mathematically related to variance (Atkins, Bohrer, et al., 2018).

Taller forests can be more complex because greater canopy volume exists in which to build structure and therefore complexity (Gough et al., 2020). In a survey of 11 temperate forested sites of the National Ecological Observatory Network (NEON) and Long-Term Ecological Research Network (LTER), Atkins, Bohrer, et al. (2018) and Atkins, Fahey, et al. (2018) found the two tallest forests—Smithsonian Environmental Research Center (SERC) in eastern MD and Great Smoky Mountains National Park (GRSM) in eastern TN—to be the most complex forests of the NEON sites surveyed in the eastern and mid-western United States. Both GRSM and SERC are older, taller forests primarily populated by deciduous broadleaf species. Gough et al. (2020), showed that canopy height (i.e. maximum canopy height or H_{Max}) was a strong predictor of complexity as estimated by the CSC metric, canopy rugosity (R_C)—an aggregate measure of horizontal and vertical variance of canopy elements. While these results indicate potential for scaling, forest type was not considered as a modifier of complexity and R_C is only one measure of complexity.

Various approaches have been used to estimate complexity since active remote sensing enabled measurement of 3D ecosystem structure in the late 1990s and early 2000s (Lefsky et al., 2002). Scores of lidar-derived structural metrics have been developed in that time, each providing insight into different facets of structure or complexity. These metrics can be broadly grouped into five categories based on structural traits of the forest and canopy they describe: (a) area and density—the distribution of photosynthetic elements in the canopy, (b) height—mean, median and maximum measures of canopy height, (c) openness and cover—openness of the planar canopy surface, (d) arrangement—relative and absolute position of canopy elements and (e) heterogeneity—the variance of canopy elements (Fahey et al., 2019). Here we compare measures of canopy height—H_{Max} and mean outer canopy height (MOCH)—to measures of canopy heterogeneity—R_C (Atkins, Bohrer, et al., 2018); foliar height diversity (FHD; MacArthur & MacArthur, 1961); and the effective number of layers (ENL; Ehbrecht et al., 2017). This combination of metrics was chosen for this analysis because they are ecologically relevant (Fahey et al., 2019), well-established in the literature (Atkins, Bohrer, et al., 2018; Ehbrecht et al., 2021) and have the potential to be estimated from different types of lidar platforms—terrestrial, UAV, aerial and spaceborne.

Here, we use a total of 1,052 terrestrial laser scanning acquisitions from 17 sites in the conterminous United States (Figure 1), covering three major forest types to test two competing hypotheses explaining height:complexity scaling. First, we hypothesize that CSC as inferred by estimates of canopy heterogeneity increases nonlinearly as a universal power law of height across forest types (H1). Tall forests will be more complex as evidenced by a shared power law relationship between measures of CSC and canopy height across all forest types. Our competing hypothesis, (H2), is that height:complexity scaling relationships will differ among forest types. Specifically, we define forest types based on plant functional types (PFTs), as described by Bonan et al. (2002). In this study, we specifically focus on deciduous broadleaf (DBF), mixed forests (MF) and evergreen needleleaf forests (ENF). We test these hypotheses by first testing for the existence of power law relationships within and across all three PFTs. We then explore two mechanisms supporting height:complexity scaling relationships: first, at the stand level, canopy layering and in-filling as inferred using a lidar-derived CSC metric (i.e. ENL); and second, at the individual level, tree architecture from the relationship between tree crown area and tree height as inferred from NEON in situ observations.

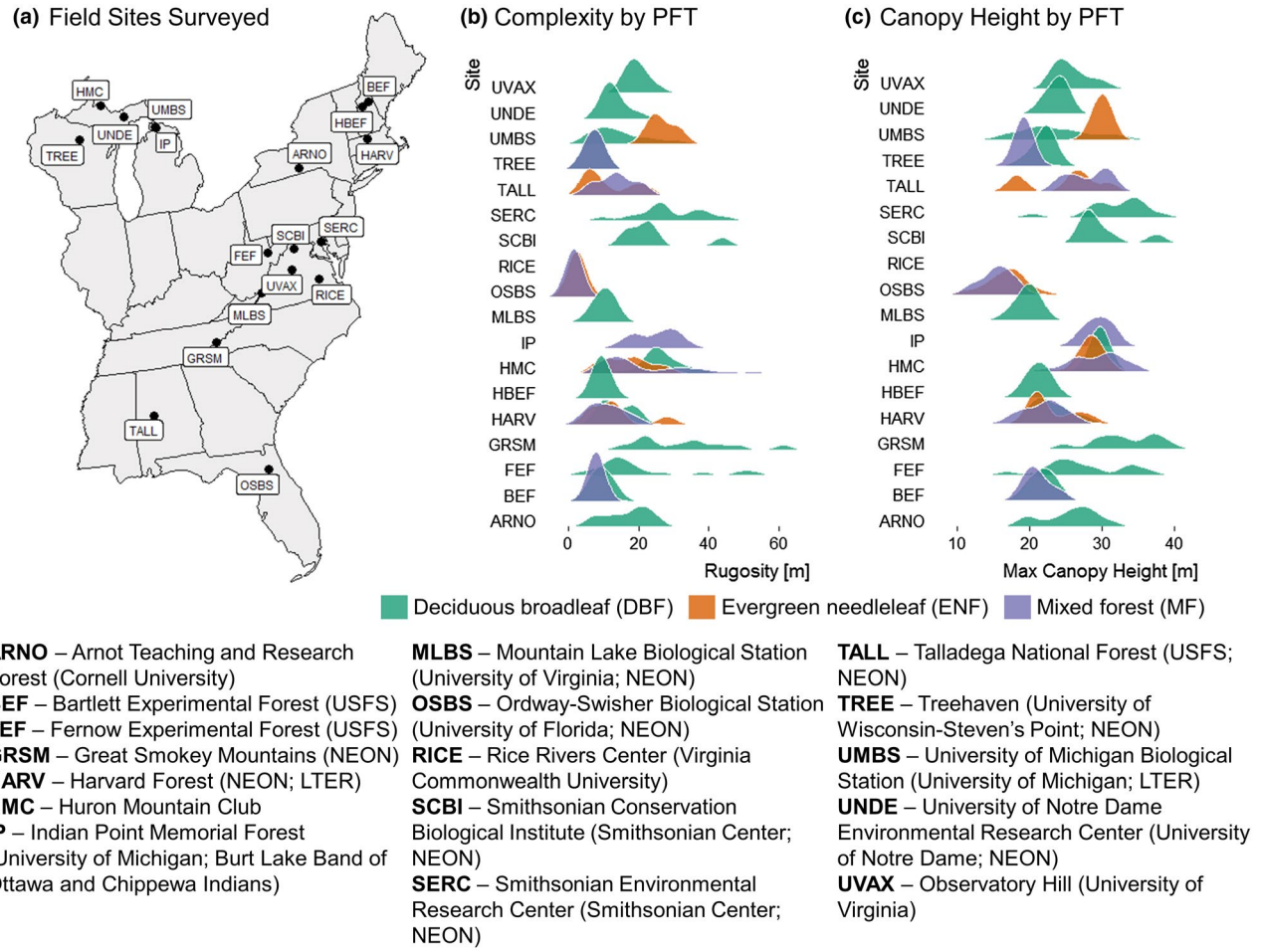

FIGURE 1 Site map showing the distribution of eastern US forests surveyed (a); distribution of complexity as measured by canopy rugosity by plant functional type (PFT) for all sites where DBF is deciduous broadleaf, (b); distribution of maximum canopy height in metres by PFT for all sites

2 | METHODS AND MATERIALS

2.1 | Datasets

We used lidar-derived CSC metrics from 484 plots, including 1,052 laser scanning acquisitions from 17 temperate forest sites, spanning a 17° latitudinal gradient across North America. These data were filtered from version 1.0 of the PCL data package (Atkins, 2021) (see data availability) which contains processed, summary statistics from lidar data collected using a 2D portable canopy lidar (PCL) system (Parker et al., 2004). The PCL system includes an upward-facing LiDAR sensor (Riegl LD-90 3100VHSFLP; Riegl USA Winter Garden) attached to a user-mounted frame moved along linear transects within a forest plot underneath the canopy. Each unique transect represents one laser scanning acquisition.

For this analysis, we included only data from 'unmanaged' plots with no recent history of disturbance and a minimum of 25% canopy cover, based on the definition of a 'forest' from Hansen et al. (2010). Canopy structural complexity (R_C, FNL and FHD) and canopy height (H_{Max} and MOCH) estimates were calculated for each laser scanning acquisition, then averaged to the plot level for a total of 484 forestry plots included in our study. Total transect length per site ranged from 240 to 10,710 m, within the range estimated by Hardiman et al. (2018) as sufficient to characterize site complexity. Limiting our data to unmanaged, undisturbed, long-term forest inventory plots insured that we were sampling contiguous, homogenous, representative forests. Each plot was classified into one of three PFTs (Bonan et al., 2002). Plots with deciduous broadleaf species encompassing 70% or more of the total basal area were classified as deciduous broadleaf forests (DBF), while plots where evergreen needleleaf trees made up greater than 70% of total basal area were classified as ENF, and all other forests were classified as MF.

Data originated from forested plots across the eastern conterminous United States (between 71° and 89° longitude), including National Ecological Observatory Network (NEON) sites, Arnot Experimental Forest, University of Michigan Biological Station (UMBS), University of Virginia Observatory Hill and Fernow Experimental Forest. Sites are described in Atkins, Fahey, et al. (2018). Other data used included another subset of data from UMBS described in Fahey et al. (2019) and data from the Huron Mountain Club described in Fahey et al. (2015b) (Table 1).

TABLE 1 Site metadata

Abbreviation	Site	Latitude	Longitude	MAT (C°)	MAP (mm)	Plant functional types (PFTs)	Total transect length (m)
ARNO	Arnot Experimental Forest, NY, USA	42.264	−76.627	9	990	DBF	2,420 ($n = 11$)
BEF	Bartlett Experimental Forest, NH, USA	44.05	−71.29	6.6	1,270	DBF	1,800 ($n = 15$)
FEF	Fernow Experimental Forest, WV, USA	39.054	−79.67	10	1,473	DBF	370 ($n = 14$)
GRSM	Great Smoky Mountain National Park, TN, USA	35.68	−72.17	13.3	1,450	DBF	1,105 ($n = 10$)
HARV	Harvard Forest, MA, USA	42.53	−72.17	8.2	1,100	DBF, ENF	3,475 ($n = 22$)
HMC	Huron Mountain Club, MI, USA	46.87	−87.891	4.2	918	DBF, ENF,MF	3,600 ($n = 75$)
HBEF	Hubbard Brook Experimental Forest, NH, USA	43.939	−71.756	5.2	1,400	DBF	3,980 ($n = 13$)
MLBS	Mountain Lake Biological Station, VA, USA	37.37	−80.52	7.8	1,250	DBF	1,250 ($n = 10$)
OSBS	Ordway-Swisher Biological Station, FL, USA	29.68	−81.99	20	1,300	ENF	2,660 ($n = 24$)
RICE	Rice Rivers Center, VA, USA	37.325	−77.206	15.5	1,140	DBF	240 ($n = 2$)
SCBI	Smithsonian Conservation Biological Institute, VA, USA	38.89	−78.14	12.5	1,050	DBF	840 ($n = 6$)
SERC	Smithsonian Environmental Research Center, MD, USA	38.88	−76.54	15	1,200	DBF	1,595 ($n = 13$)
TALL	Talladega National Forest, AL, USA	32.95	−87.39	17	1,400	MF	1,450 ($n = 12$)
TREE	Treehaven, WI, USA	45.49	−89.58	5.4	800	MF	1,250 ($n = 10$)
UMBS	University of Michigan Biological Station	45.55	−84.7	5.5	817	DBF, MF	10,710 ($n = 215$)
UNDE	University of Notre Dame Environmental Research Center, WI/MI, USA	46.23	−86.54	4.5	800	DBF	1,255 ($n = 9$)
UVAX	Observatory Hill, VA, USA	38.034	−78.524	13.15	1,143	DBF	800 ($n = 9$)

2.2 | Power law scaling

We chose three CSC metrics describing canopy heterogeneity as defined by the framework established by Atkins, Bohrer, et al. (2018) and amended by Fahey et al. (2019): R_C, an aggregate measure of horizontal and vertical variance of plant area density (Atkins, Bohrer, et al., 2018); FHD, an application of Shannon–Weiner diversity to the vertical distribution of canopy leaf area (MacArthur & MacArthur, 1961); and the ENL, a measure of canopy layering based on the filling of defined 1 m canopy layers (Ehbrecht et al., 2017). FHD, ENL and R_C may be partially correlated across forests, yet each describe different, though related, facets of canopy complexity.

To analyse scaling relationships between canopy height and each metric, we used two different measures of canopy height: H_{Max}, the highest measured lidar return for each laser scanning acquisition within the plot; and MOCH, the mean of the highest measured lidar returns for each equally spaced, 1 m section of linear transect distance (Figure 1). This approach was taken to account for different methods defining a forest canopy. Using H_{Max} to define the canopy includes all the 'potential' space for foliar elements but could be biased in plots where there are emergent individuals that are significantly taller than their neighbours, while MOCH approximates the average canopy space, but could be biased lower in areas where there is dense understorey that increases occlusion—when laser pulses from terrestrial-based instrumentation fail to sufficiently reach the upper regions of the canopy. MOCH scales linearly with H_{Max} (Figure S2).

We took the base-10 logarithm of each metric to stabilize the variances and allow for the assessment of whether the relationship between each heterogeneity and height metric was best described by a power law. The power law relationship:

$$\mathrm{CSC}_i = aH_j^b, \tag{1}$$

where H_j is a height metric, CSC_i is a structural metric and a and b are the power law coefficients, and CSC_i was linearized by taking the base-10 logarithm of each side:

$$\log_{10}\left(\mathrm{CSC}_i\right) = \log_{10}(a) + b\log_{10}\left(H_j\right). \tag{2}$$

We then used ordinary least squares (OLS) regression to estimate $\log_{10}(a)$ and b, quantifying the relationship between each height and heterogeneity metric. We deemed OLS regression appropriate for this analysis over Model II regression (i.e. reduced major axis or

RMA regression) for two reasons. First, the uncertainty associated with estimating canopy complexity is greater than that of estimating height. Model II regression methods assume symmetry in the uncertainty in the relationship between *x* and *y*, but this is likely not the case. Second, there is no standard multiple regression method for Model II regression, thus preventing the appropriate diagnostics (see next paragraph) to determine whether these relationships are well-described by a power law. However, for comparison, we also computed relationships using RMA regression, and these generally were consistent with OLS estimates and are included in Table S1.

We tested whether the data were well-described by a power law by evaluating the linearity and homoscedasticity of each log-transformed relationship, following Zhao et al. (2019). The linearity criterion was evaluated by comparing the fit of the linear model to that of a quadratic model [i.e. $\log_{10}(CSC_i) = \log_{10}(a) + b_1\log_{10}(H_j) + b_2\log_{10}(H_j)^2$] using a likelihood ratio test. The homoscedasticity criterion was evaluated by testing for a statistically significant relationship between $\log_{10}$(CSC) and the absolute-valued residuals from the linear model (Equation 2). Because we were interested in general empirical relationships and willing to accept the hypothesis that the canopy height–CSC relationship is approximately a power law unless there were considerable deviations, we used a type-1 error rate of $\alpha = 0.1$ for both diagnostic criteria. If both diagnostic criteria were passed, we then used the 95% confidence interval on the estimate of *b* to assess whether it is different from 1 (Walter et al., 2020). Super-linear slopes ($b > 1$) indicate that complexity increases more rapidly than height as height increases, while sublinear slopes indicate that height increases more rapidly than complexity as height increases.

We fit linearized power law functions and performed diagnostic tests with data pooled across all plots and separately by PFT: DBF, ENF and MF. Using the pooled data, we conducted a statistical test for differences by PFT in the slopes and intercepts of height:complexity relationships using OLS linear models in R 4.03 (R Core Team, 2020) using type III errors from the CAR package (Fox et al., 2021). We tested for effects of height, forest type and height:-forest type interaction on complexity. We interpreted a significant forest type effect as evidence that the coefficient *a* depends on forest type, and a significant height:forest type interaction term as evidence that the exponent (or slope on the log-log scale) *b* depends on forest type. Again, where forest type is the relevant plant functional type or PFT (e.g. deciduous broadleaf, evergreen needleleaf). Statistical significance was assessed at $\alpha = 0.05$. Post hoc Tukey's HSD tests were used to determine which forest types differed statistically. However, we used simple OLS fits of Equation (2) to data separated by forest type for parameter estimation and for plotting relationships.

2.3 | Potential mechanism 1: Canopy layering and in-filling

We first explored differences in stand-scale canopy layering and in-filling as they relate to canopy height among forest types as a potential mechanism underlying height:complexity scaling relationships. We used natural scale values of ENL as an analogue for canopy layering and in-filling. ENL approximates the number of 1-m thick vegetation layers within a canopy. We used linear regression analysis with natural scale values of ENL and H_{Max} to explore differences in how canopy layering developed with height as measured by H_{Max} among broadleaf, needleleaf and MF. The slope of the linear relationship approximates the rate at which canopy layers develop per 1 m unit of height, providing a potential mechanism at the plot to stand level explaining scaling relationships among forest types. A relatively shallower slope for a given forest type will indicate that layering develops slowly with height, while a relatively steeper slope will indicate layering develops more rapidly.

2.4 | Potential mechanism 2: Tree architecture

In addition to exploring mechanisms underlying height:complexity scaling relationships at the stand scale, we examined whether mean crown area of individual trees scales with tree height. We used linear regression analysis on $\log_{10}$-transformed crown area and $\log_{10}$-transformed tree height data of 6,457 individual trees from 22 field sites in the NEON vegetation database to test for relationships at the individual tree level, specifically if crown area scales with tree height differently in broadleaf versus needleleaf tree species. Differences in the slope and intercepts of crown area to height relationships were analysed using analysis of covariance (ANCOVA) in R 4.03 (R Core Team, 2020) using type III errors from the CAR package (Fox et al., 2021). More specifically, we tested for effects of log(height), forest type and log(height):forest type. Differences in the regression slopes between broadleaf and needleleaf species could provide a potential mechanism at the individual level explaining scaling relationships. Individual tree NEON tree data were acquired from the NEON data portal using vegetation survey data for years 2015–2019 (National Ecological Observatory Network (NEON), 2021). NEON sites used for this analysis include: ABBY—Abby Road, Washington, USA; BLAN—Blandy Experimental Farm, Virginia, USA; DEAL—Dead Lake, Alabama, USA; DEJU—Delta Junction, Arkansas, USA; DSNY—Disney Wilderness Preserve, Florida; GUAN—Guanica Forest, Puerto Rico, USA; HARV—Harvard Forest, Massachusetts, USA; KONZ—Konza Prairie, Kansas, USA; LAJA—Lajas Experimental Station, Puerto Rico, USA; MLBS—Mountain Lake Biological Station, Virginia, USA; MOAB—Moab, Utah, USA; NIWO—Niwot Ridge, Colorado, USA; ORNL—Oak Ridge National Laboratory, Tennessee, USA; RMNP—Rocky Mountains, Colorado, USA; SOAP—Soaproot Saddle, California, USA; SCBI—Smithsonian Conservation Biological Institute, Virginia, USA; SERC—Smithsonian Environmental Research Center, Maryland, USA; SJER—San Joaquin Experimental Range, California, USA; TREE—Treehaven, Wisconsin, USA; UKFS—University of Kansas Field Station, Kansas, USA; WREF—Wind River Experimental Forest, Washington, USA; and YELL—Yellowstone National Park, Wyoming, USA.

3 | RESULTS

The interpretation of our results relies upon an understanding of power law scaling relationships. Power laws can either be 1:1, where the slope (*b*) is approximately 1; sublinear, where the slope is less than 1; or super-linear, where the slope is >1. A sublinear power law indicates that complexity scales at less than a rate of 1 to 1 with canopy height, while a super-linear relationship indicates complexity scales greater than 1 to 1 with height. A 1:1 power law relationship indicates that complexity and canopy height scale in tandem (see Table S1).

3.1 | Power law scaling—Canopy rugosity (R_C)

Among all forest types, neither the relationship between R_C and H_{Max}, or R_C and MOCH was best described by a power law despite statistical significance as indicated by OLS regression results (Table S1). Within forest types, we found evidence for power law relationships within some combinations of R_C and either/or H_{Max} and MOCH. For broadleaf forests, the R_C to H_{Max} relationship was a super-linear power law ($a = 2.30 \pm 0.19$; $b = 2.50 \pm 0.13$; where a is the intercept and b is the slope of the relationship and $\pm$ error is the 95% confidence interval); for needleleaf forests both the R_C to H_{Max} ($a = -3.69 \pm 0.58$; $b = 3.37 \pm 0.43$) and R_C to MOCH relationships ($a = -1.57 \pm 0.40$; $b = 2.26 \pm 0.36$) were super-linear power laws; and for MF, both the R_C to H_{Max} ($a = -3.66 \pm 0.55$; $b = 3.40 \pm 0.39$) and R_C to MOCH relationships ($a = -1.28 \pm 0.35$; $b = 2.030 \pm 0.193$)) were super-linear power laws.

The slopes of the H_{Max} to R_C relationships (Figure 2a) were significantly different by forest type based on ANCOVA results (Table 2) with pairwise comparisons showing differences among all forest types ($p = <0.001$). No differences were found among forest types when comparing the R_C to MOCH relationships (Table 2).

3.2 | Power law scaling—ENL

Among all forest types, no relationships between ENL and either H_{Max} or MOCH were best described by a power law (Table S1). Within forest types, the ENL to H_{Max} relationships for broadleaf forests ($a = 0.02 \pm 0.11$; $b = 0.88 \pm 0.08$) and MF ($a = -0.20 \pm 0.25$;

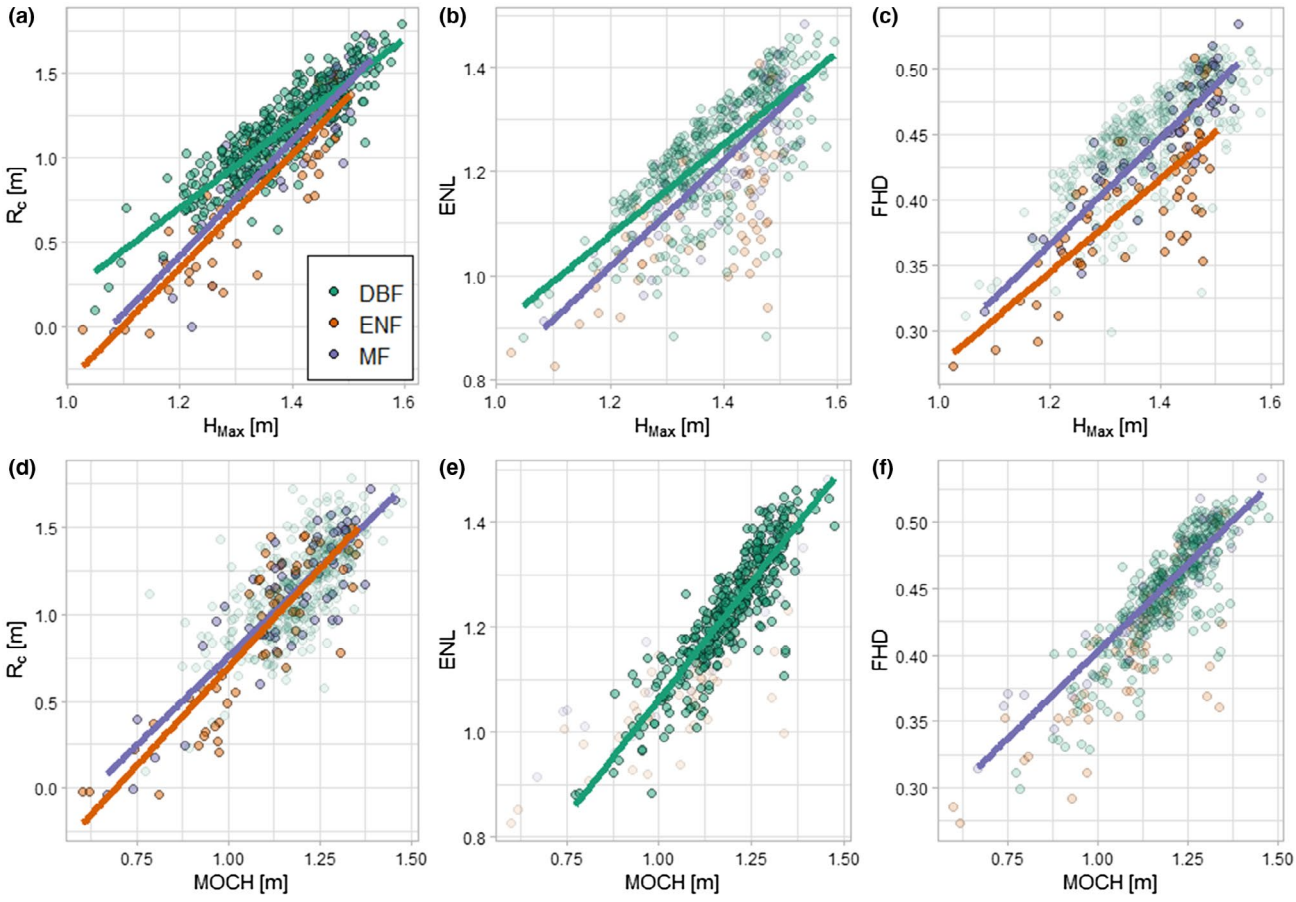

FIGURE 2 Log_{10}–log_{10} relationships between maximum canopy height (H_{Max}) and mean outer canopy height (MOCH) and (a, d) canopy rugosity (R_C), (b, e) the effective number of layers (ENL) and (c, f) foliar height diversity (FHD). Data are coloured by plant functional type (i.e. forest type) as defined by Bonan et al. (2002): deciduous broadleaf forests (DBF); mixed forests (MF); and evergreen needleleaf forests (ENF). Regression lines indicate power law relationships (Table S1), whereas the absence of regression lines and the semi-transparence of data values represent relationships not well-described by a power law

TABLE 2 ANCOVA results for differences among regression slopes by forest type (PFT) where SS is sum of squares, MS is mean squares, *F* is the *F* statistic and *p* is the *p*-value where significance is based on an alpha of 0.05

Model		SS	MS	*F*	*p*
$\log_{10}(\text{ENL}) \sim \log_{10}(H_{Max}) \times \text{PFT}$	$\log_{10}(H_{Max})$	3.75	3.75	609.89	«0.001
	PFT	0.64	0.32	52.52	«0.001
	$\log_{10}(H_{Max})$: PFT	0.04	0.02	3.04	0.048
$\log_{10}(FHD) \sim \log_{10}(H_{Max}) \times \text{PFT}$	$\log_{10}(H_{Max})$	0.55	0.55	777.35	«0.001
	PFT	0.08	0.04	57.86	«0.001
	$\log_{10}(H_{Max})$: PFT	< 0.01	<0.01	3.68	0.025
$\log_{10}(R_C) \sim \log_{10}(H_{Max}) \times \text{PFT}$	$\log_{10}(H_{Max})$	37.39	37.39	1,907.48	«0.001
	PFT	2.49	1.25	63.53	«0.001
	$\log_{10}(H_{Max})$: PFT	0.8	0.40	20.47	«0.001
$\log_{10}(\text{ENL}) \sim \log_{10}(\text{MOCH}) \times \text{PFT}$	$\log_{10}(\text{MOCH})$	5.578	5.578	1,703.81	«0.001
	PFT	0.106	0.053	16.20	«0.001
	$\log_{10}(\text{MOCH})$: PFT	0.128	0.064	19.59	«0.001
$\log_{10}(\text{FHD}) \sim \log_{10}(\text{MOCH}) \times \text{PFT}$	$\log_{10}(\text{MOCH})$	0.72	0.72	1,445.77	«0.001
	PFT	0.016	0.008	16.39	«0.001
	$\log_{10}(\text{MOCH})$: PFT	0.002	0.001	2.58	0.07
$\log_{10}(R_C) \sim \log_{10}(\text{MOCH}) \times \text{PFT}$	$\log_{10}(\text{MOCH})$	30.95	30.95	801.21	«0.001
	PFT	0.177	0.089	5.72	0.10
	$\log_{10}(\text{MOCH})$: PFT	0.44	0.22	5.73	0.003

$b = 1.02 \pm 0.17$) were best described as sublinear and 1:1 power laws respectively. The ENL to MOCH relationships in broadleaf forests ($a = 0.17 \pm 0.13$; $b = 0.89 \pm 0.04$) were best described as a sublinear power law.

We observed significant differences among the slopes and intercept of the relationship between ENL and H_{Max} based on ANCOVA results, with pairwise comparisons showing differences among forest types. We also observed differences among the ENL to MOCH relationship among forest, though pairwise comparisons showed only that needleleaf forests differed from broadleaf forests and MF (Figure 2c; Table 2).

3.3 | Foliar height diversity

Among all forest types, we found significant relationships between FHD and both H_{Max} and MOCH, yet only the FHD to MOCH relationship was best described by a power law ($a = 0.097 \pm 0.01$; $b = 0.29 \pm 0.02$). Within forest types, we found evidence for power law relationships within some combinations of FHD to H_{Max}. Needleleaf forests ($a = 0.08 \pm 0.05$; $b = 0.35 \pm 0.08$) and MF ($a = -0.12 \pm 0.07$; $b = 0.40 \pm 0.04$) were both best described as sublinear power laws. In MF, the FHD to MOCH relationship was also a sublinear power law ($a = 0.13 \pm 0.03$; $b = 0.26 \pm 0.03$).

There were significant differences in the slopes of the relationship between FHD and H_{Max} by forest type with pairwise comparisons showing these differences arose from significant differences between needleleaf and broadleaf forests, and needleleaf forests and MF (Figure 2b; Table 2). Broadleaf forests and MF were not statistically different.

3.4 | Mechanism 1: Canopy layering and in-filling

While not every relationship between our measures of canopy height and measures of CSC was best described by power laws, we did find that the slopes of the relationships between all combinations of variables (except for R_C and MOCH) significantly differed among forest types based on ANCOVA results (Table 2). Pairwise comparisons of these results showed that for every combination of forest type (e.g. broadleaf to needleleaf and mixed to broadleaf), that the slope of the relationships between H_{Max} to both R_C and the ENL was significantly different. These findings provide evidence supporting our first proposed mechanism underlying height:complexity relationships, that forest types differ in the rate or amount of canopy layering and in-filling that occurs with height. We can use ENL—which estimates the number of distinct 1-m thick layers within the canopy—as an estimate of canopy layering. When analysed using natural scale values, ENL (Ehbrecht et al., 2017) increased at a rate of 0.42 layers per metre of height for needleleaf forests ($\text{ENL} = 0.42H_{Max} + 3.33$; $R^2 = 0.36$) as compared to greater rates of increase in broadleaf forests ($\text{ENL} = 0.63H_{Max} + 2.27$; $R^2 = 0.56$) and MF ($\text{ENL} = 0.72H_{Max} - 1.27$; $R^2 = 0.63$). This shows us that needleleaf forests created canopy layers at approximately two thirds the rate of either mixed or broadleaf forests based on the slopes of these linear relationships (Figure 3).

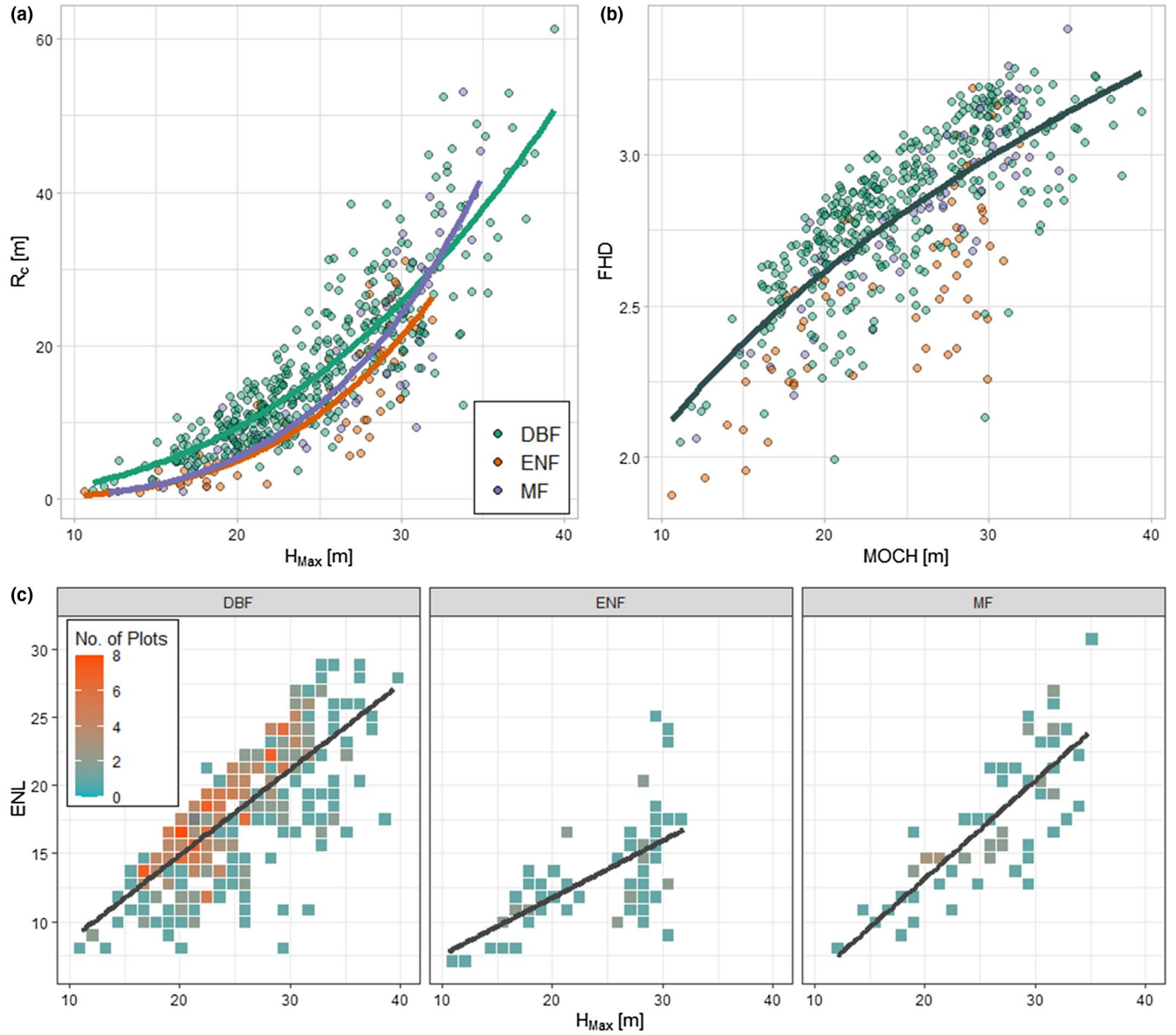

FIGURE 3 Using natural scale data, we see canopy complexity increased with height for all PFTs, but more slowly for needleleaf forests (ENF) and mixed forests (MF) (a); FHD scaled with MOCH across all PFTs (b). At bottom (c), as measured by ENL, canopy layering increased at a rate of 0.42 layers per metre of height for ENF (ENL = $0.42H_{Max} + 3.33$; $R^2 = 0.36$) as compared to either broadleaf (DBF) (ENL = $0.63H_{Max} + 2.27$; $R^2 = 0.56$) or mixed forests (MF) (ENL = $0.72H_{Max} - 1.27$; $R^2 = 0.63$). Linear regression analysis demonstrated differences among PFTs in canopy layering by height. All statistical relationships were significant at alpha = 0.05. Relationships between both needleleaf forests and MF and H_{Max} were well-described by power law functions, but broadleaf forests did not demonstrate power law relationships between ENL and H_{Max}. Pairwise comparisons of natural scale data showed that needleleaf forests are the only forests to differ statistically from others

3.5 | Mechanism 2: Crown architecture

We found support for our second proposed mechanism underlying canopy height:complexity relationships that individual tree height:canopy area ratios differ between needleleaf and broadleaf species An analysis of 6,457 individual trees from 22 field sites in the NEON vegetation database comparing individual measured tree height with modelled tree crown area shows that patterns at the individual tree level mirror those observed in our analysis at the plot to site level—with crown area increasing with tree height in an approximate power law. Linear regression analysis of crown area to tree height was statistically significant for both needleleaf ($R^2 = 0.75$; $p = « 0.001$) and broadleaf ($R^2 = 0.64$; $p = «0.001$) species. ANCOVA results show the slope of these relationships significantly differ ($p = «0.0001$).

4 | DISCUSSION

We illustrated generalizable mathematical relationships linking forest canopy height—easily measured using aerial and satellite

remote sensing—with CSC, which has been strongly tied to ecosystem functioning and habitat value. We have shown the relationship between canopy height and the emergent property of interior CSC can be described by power laws. The universality and scale invariance of power laws are inherently beneficial to understanding fundamental processes in ecology (Farrior et al., 2016; Marquet et al., 2005; Stark et al., 2015) and the relationships identified here likely reflect fundamental ecological processes related to canopy space filling and optimization of light capture (Anten, 2016; McMahon, 1973). While we framed our hypotheses as opposing—that power law relationships are generalizable across all forests (H1) or, alternatively, are forest type specific (H2), our findings indicated support for both hypotheses, depending on which conceptions of height and complexity were compared. When canopy height is expressed as a mean or composite value (e.g. MOCH), we found a universal relationship with canopy complexity as measured by FHD across all forest types. However, when we measured canopy height as a maximum or peak value (e.g. H_{Max}), there were no longer common relationships across forest types. We observed DBF had initially higher values of CSC for a given height as compared to either MF or ENF, but that complexity increased at a lower rate with height for broadleaf forests than it did for either MF or needleleaf forests. We attributed differences among forest types in power law relationships between height and complexity to differences in tree architecture among species, as well as canopy layer development, successional processes and competitive exclusion.

4.1 | Scaling across all forest types

A strong universal power law relationship existed between complexity measured as FHD and canopy height as measured by MOCH among all forest types surveyed. FHD is calculated as a sum over vertical canopy strata (Table 3) so it follows that FHD increases with canopy height, although a power law is not mathematically guaranteed. FHD can be remotely sensed from lidar sensors aboard ground, air- and spaceborne platforms, including NASA's Global Ecosystem Dynamics Investigation (GEDI; Dubayah et al., 2020). GEDI does not, however, provide wall-to-wall estimates of FHD—FHD and other complexity/structure metrics available from GEDI are calculated at the waveform level. The strong correlation we observed between FHD and MOCH indicates the potential to infer FHD (i.e. complexity) from canopy height models, which are more widely available than lidar point clouds and computationally simpler to analyse. The key advantage to our approach using terrestrial lidar is the ability of terrestrial-based sensors to provide greater intra-canopy detail than air- or spaceborne sensors.

4.2 | Scaling within PFTs

Needleleaf forests initially developed less complexity per unit height than either broadleaf or mixed forests, but as forest height increased past some threshold, needleleaf forests developed complexity at rates greater than other forest types. Our data showed these trends converged at around 35 m in height (Figure 3). Consistent with these findings, Fahey et al. (2015a) showed that broadleaf forests (i.e. sugar maple dominated in their analysis) were 10 m taller but nearly four times more complex than similarly aged needleleaf (hemlock dominated) stands in the upper peninsula of Michigan. Correspondingly, Wales et al. (2020) found similarly aged needleleaf forests were significantly less complex than either broadleaf or mixed stands. However, our analysis did not include forests over 40 m because of limited terrestrial lidar-derived complexity data for these forests. If we extrapolate from our findings, we can hypothesize two possible trajectories for complexity

TABLE 3 Canopy structural complexity heterogeneity metrics

Metric	Acronym	Formula	Definition
Canopy rugosity	R_C	$R_C = \left[\frac{\sigma_H^2}{L_T} - \left(\frac{\sigma_H}{L_T}\right)^2\right]^{0.5}$	R_C is the accumulated variance of leaf area/leaf area density in both horizontal and vertical directions in units of metres. In the equation at left, of each plot was calculated from the transect-long (L_T), standard deviation (σ) in column vegetation area index (VAI)-weighted mean heights (H) (Atkins, Bohrer, et al., 2018; Gough et al., 2020; Hardiman et al., 2013)
Foliar height diversity	FHD	$FHD = \sum_{i=1}^{n} \rho_i \times \log\rho_i$	FHD was codified by MacArthur and MacArthur (1961), and is the distribution of canopy cover among forest strata or layers expressed as a diversity index. FHD is dimensionless. In the equation at left, ρ_i is the proportion of leaf area density in each layer i
Effective number of layers	ENL	$ENL = 1/\sum_{i=1}^{n} \rho_i^2$	ENL, like FHD, quantifies the distribution of leaf area/leaf area density through the canopy but is based on the occupation of 1-m wide vertical layers by tree components relative to the total space occupation of a stand. ENL is in units of metres. In the equation at left, n is the number of 1-m thick canopy layers, and ρ_i is the proportion of filled voxels in each layer i (Ehbrecht et al., 2017)

and height relationships for very tall forests. Either complexity saturates with height for all PFTs at a certain threshold, potentially in the 35–45 m height range, or needleleaf forests continue to increase in complexity at a greater rate per unit height than either broadleaf or MF (Figure S2).

4.3 | Canopy layering and crown architecture

We hypothesized that tree architectural constraints likely influenced the initial lower rate of complexification of needleleaf forests with height, relative to broadleaf forests or MF. Needleleaf species may have fewer available canopy topologies than broadleaf species resulting in simply fewer relative ways to 'build' a tree (Verbeeck et al., 2019). With fewer building blocks, the number of possible structural configurations is reduced, limiting complexity. At the level of the individual tree, canopy topology, or crown form, arises from internal branching topology, which is primarily constrained by genetics, light availability and hydraulics (Horn, 1971). An explicitly trait-based approach in the future research could be incredibly beneficial in understanding and predicting functional outcomes by considering the properties of the individual (Enquist et al., 2015). The excurrent growth forms of many needleleaf species, as compared to decurrent growth forms of broadleaf species, may also be a geometrically limiting factor. The greatest diversity in crown architectures occurs in the tropics due to interspecific competition arising from spatial and temporal climate similarity creating uniformly favourable growth conditions (Tomlinson, 1987). Underlying branching topology—again, primarily constrained by light and water availability—appears to have little to no effect on differences in crown form in highly biodiverse tropical forests (Martin-Ducup et al., 2020), as neither water nor light are limiting. In these systems, successional events, gap-formation processes and available canopy space are stronger predictors of crown form (Hallé et al., 1978; Martin-Ducup et al., 2020). In temperate and boreal forests however, climate is far more seasonal and variable, resulting in greater competition for light and water, creating fewer potential crown topologies, and limiting the number of possible structural configurations. Ehbrecht et al. (2021) showed that potential forest complexity declined with increasing latitude in the northern hemisphere which may be attributable to how needleleaf trees supplant broadleaf trees with increasing latitude and elevation in part because they are more resistant to xylem cavitation and more efficient at utilizing diffuse light, allowing them to live in colder environments than many broadleaf species can tolerate. Correspondingly, boreal forests have lower species richness and shorter average canopy heights—patterns also observable with increasing elevation.

At the individual tree level, needleleaf species create more compact, denser crowns than broadleaf species (Sprugel, 1989) and tend to be more conical in their architecture—broader at crown base than at crown top—the opposite of many broadleaf species. While these differences are manifested at the individual level, we note our study assessed the layering of the entire canopy. At the canopy or stand level then, the higher rate of layering we observed in broadleaf forests may be a product of greater competition for light with multiple individuals competing by filling different canopy layers. The decreased rate of layering in needleleaf forests therefore is likely a product of reduced competition for light among individuals. Needleleaf species maximize light capture at the leaf level—the cylindrical shape of needles is more efficient at capturing diffuse light—as well as at the individual level—creating denser crowns than broadleaf species. Needle leaves also have higher leaf mass per area and longer life spans than broad leaves, indicative of the higher resource investment made by needleleaf species (Wright et al., 2004). These crown structural and architectural adaptations also help needleleaf species to enhance carbon gain during the growing season and survive harsher winter conditions (Smith & Brewer, 1994). This suggests that there may be less canopy overlap in needleleaf forests than in forests where broadleaf species are dominant.

We found broadleaf species produced greater crown area at lower heights, with the ratio of crown area to height converging as height increased for needleleaf species. (Figure 4a)—a relationship conserved across elevation (Figure 4b) which provides additional confidence in our findings regarding differences in height:complexity scaling among PFTs, implying the pattern we observed is not a result of environmental gradients. Crown area to height for needleleaf species does appear to be more variable with increasing latitude than it does for broadleaf species which supports findings from Ehbrecht et al. (2021). However, sub-boreal and boreal forests are not well-represented in this dataset, possibly limiting the scope of inference. The availability of forest structural complexity data across broader areas (e.g. NASA's GEDI and ICESat2 missions) will help to address to fill this niche and further allow us to test the universality of the scaling relationships we observed.

4.4 | Height and canopy volume

The difference in the relationship between CSC and different measures of height—either MOCH or H_{Max}—also make us consider how we conceptualize canopy or stand height. The height of a tree is a measurable attribute. Beyond the individual, the concept of height becomes difficult to define. As Gough et al. (2020) describe, height creates the upper bound on the forest canopy, with the space beneath being the volume in which complexity emerges. We can then think of all canopy elements that fill this space as 'building blocks' to be arranged. While a full consideration of how the upper limit of the canopy is defined is outside the focus of this paper, we consider that H_{Max} is the upper limit of the canopy volume while MOCH describes the average canopy state. How best to define canopy height, conceptually or practically, is potentially less well-resolved than traditional wisdom implies.

We found R_C had a power law relationship with H_{Max} within each forest type grouping, but not across all forests. This further supports the finding that there are differences in in how complexity arises within each forest type—or in how we currently estimate

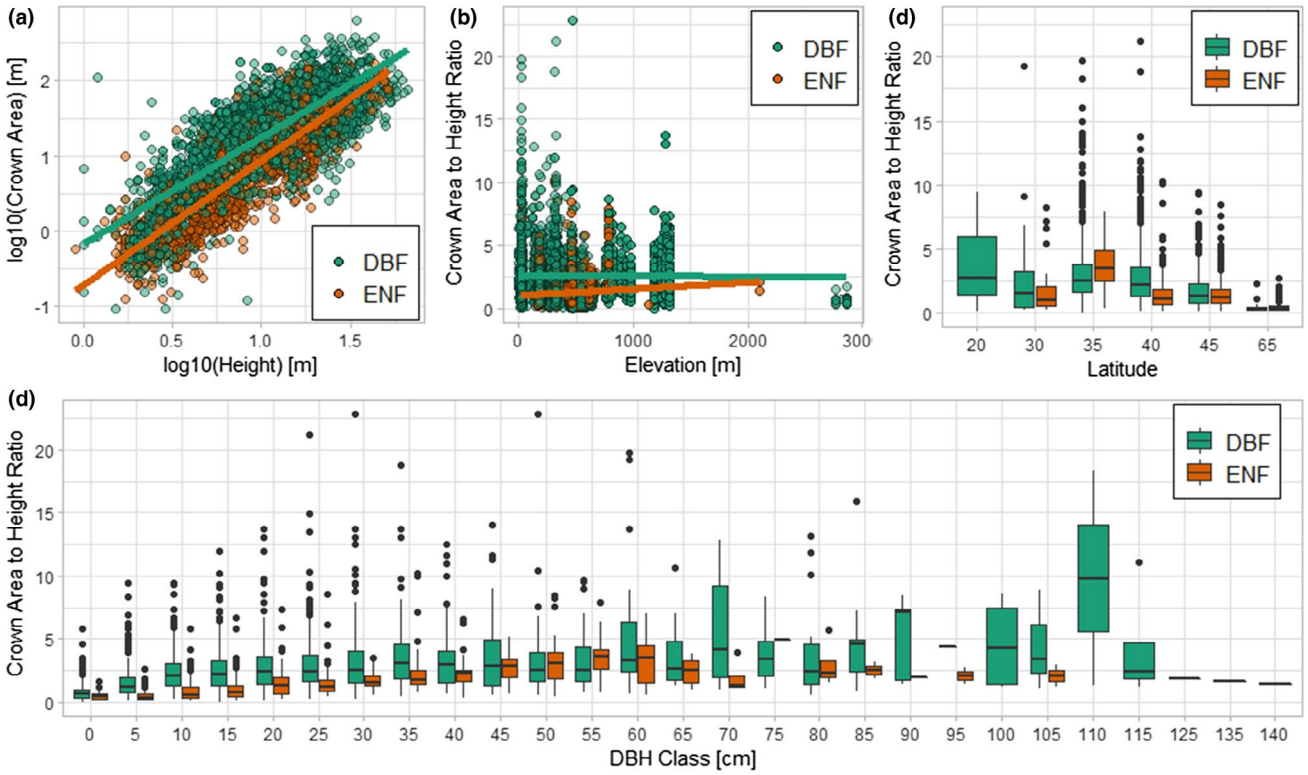

FIGURE 4 Comparison of individual measured tree height and crown area from 6,547 trees in the NEON database from 22 NEON field sites across the conterminous United States and Puerto Rico

complexity. Though the general form of the relationships is that of a power law, the scaling factors of those relationships differ. For both broadleaf and mixed forests, where R_C power law relationships existed for both H_{Max} and MOCH relationships, the slopes of those relationships were higher for H_{Max} (DBF, $b = 2.53$; MF, $b = 2.62$) than they were for MOCH (DBF, $b = 1.4$; MF, $b = 1.28$). H_{Max} as a maximum value and by definition greater than MOCH. However, given that complexity increases with H_{Max} at 1.8–2 times the rate it does with MOCH, this is an important consideration when inferring complexity from height data.

4.5 | Implications for measurement, research and management

The universality of power law relationships extends our potential to broadly estimate and model CSC—and associated functional and habitat values. With the increasing use of terrestrial, aerial, and spaceborne laser scanning (Calders et al., 2020; Dubayah et al., 2020), we are expanding our understanding of the role of forest and CSC. As our understanding of complexity scaling evolves, we can further incorporate complexity into restoration and silvicultural practice, promoting adaptability and resilience (Fahey et al., 2018). In this paper, we have shown that scaling relationships between forest height and complexity are nonlinear. This is important as understanding the mathematical form of forest height:complexity relationships can better inform applications seeking to estimate fundamental forest attributes and processes including standing biomass, carbon sequestration, element cycling and biodiversity.

We are witnessing a revolution in our understanding of the structural diversity of ecosystems—its fundamental nature, how it is measured and the role complexity plays in ecosystem functioning and habitat provisioning. This revolution is driven by theoretical advances such as power law scaling relationships shown here as well as our growing understanding of the role of landscape and climate in shaping forest structure (Ehbrecht et al., 2021). Height dependency relationships have already been used to inform management decisions: when canopy density is modelled with stand height, predictions of stand volume improve (Xu et al., 2019). Here we have shown there is ever greater potential. Canopy structural complexity metrics are strong information aggregators; mechanistically, this is due in part to their strong height dependency as well as their correlations with leaf area, biomass and biodiversity—additional factors that in combination constrain function. Canopy structural complexity metrics aggregate structural and compositional characteristics, and thus become, both figuratively and mathematically, greater than the sum of their parts.

ACKNOWLEDGEMENTS

This work was supported by the National Science Foundation's Division of Emerging Frontiers, Awards 1550657 (CMG, JWA), 1550650 (RTF) and 1550639; and the NASA Postdoctoral Program Fellowship (AELS). We would like to thank Courtney Meier and NEON Inc. for data and logistical support. We also wish to acknowledge the

valuable feedback provided by Associate Editor Dr. Sayer and two anonymous reviewers, and thank them for their time and effort.

The research areas surveyed in this manuscript are located on unceded lands of the Chippewa, Choctaw, Creek, Manahoac, Massawomeck, Menominee, Monacan, Muscogee, Odawa Anishinabewaki, Powahatan, Tutelo, Seminole, Susquehannock, Tsalaguwetiyi/Eastern Band of the Cherokee, and Wabanaki, respectively. We acknowledge the forced removal of these peoples from their ancestral lands by white settlers and colonizers. The reputations and esteem of institutions built on these lands are rooted in the erasure and exclusion of Indigenous peoples. We recognize these peoples as the traditional stewards of their ancestral lands and wish to acknowledge their continuing presence and enduring cultural legacies.

CONFLICT OF INTEREST

The authors collectively and individually declare no competing interests.

AUTHORS' CONTRIBUTIONS

J.W.A. conceived the project and wrote the paper; J.W.A., J.A.W. and A.E.L.S. performed the analyses. All authors contributed to writing and revising the paper.

DATA AVAILABILITY STATEMENT

All data are deposited in Zenodo https://doi.org/10.5281/zenodo.5764251 (Atkins, 2021).

ORCID

Jeff W. Atkins https://orcid.org/0000-0002-2295-3131
Jonathan A. Walter https://orcid.org/0000-0003-2983-751X
Atticus E. L. Stovall https://orcid.org/0000-0001-9512-3318
Robert T. Fahey https://orcid.org/0000-0001-7246-8292
Christopher M. Gough https://orcid.org/0000-0002-1227-7731

REFERENCES

Aber, J. D., Pastor, J., & Melillo, J. M. (1982). Changes in forest canopy structure along a site quality gradient in Southern Wisconsin. *The American Midland Naturalist*, *108*(2), 256–265. https://doi.org/10.2307/2425486

Anten, N. P. R. (2016). Optimization and game theory in canopy models. In K. Hikosaka, Ü. Niinemets, & N. P. R. Anten (Eds.), *Canopy photosynthesis: From basics to applications* (pp. 355–377). Springer. https://doi.org/10.1007/978-94-017-7291-4_13

Atkins, J.. (2021). atkinsjeff/csc_powerlaw: CSC Power-Law scaling (v1.0.1). *Zenodo*, https://doi.org/10.5281/zenodo.5764251

Atkins, J. W., Bohrer, G., Fahey, R. T., Hardiman, B. S., Morin, T. H., Stovall, A. E. L., Zimmerman, N., & Gough, C. M. (2018). Quantifying vegetation and canopy structural complexity from terrestrial LiDAR data using the forestr r package. *Methods in Ecology and Evolution*, *9*(10), 2057–2066. https://doi.org/10.1111/2041-210X.13061

Atkins, J. W., Fahey, R. T., Hardiman, B. S., & Gough, C. M. (2018). Forest canopy structural complexity and light absorption relationships at the subcontinental scale. *Journal of Geophysical Research: Biogeosciences*, *123*(4), 1387–1405. https://doi.org/10.1002/2017JG004256

Bonan, G. B., Levis, S., Kergoat, L., & Oleson, K. W. (2002). Landscapes as patches of plant functional types: An integrating concept for climate and ecosystem models. *Global Biogeochemical Cycles*, *16*(2), 5–1-5–23. https://doi.org/10.1029/2000GB001360

Calders, K., Adams, J., Armston, J., Bartholomeus, H., Bauwens, S., Bentley, L. P., Chave, J., Danson, F. M., Demol, M., Disney, M., Gaulton, R., Krishna Moorthy, S. M., Levick, S. R., Saarinen, N., Schaaf, C., Stovall, A., Terryn, L., Wilkes, P., & Verbeeck, H. (2020). Terrestrial laser scanning in forest ecology: Expanding the horizon. *Remote Sensing of Environment*, *251*, 112102. https://doi.org/10.1016/j.rse.2020.112102

Davies, A. B., Ancrenaz, M., Oram, F., & Asner, G. P. (2017). Canopy structure drives orangutan habitat selection in disturbed Bornean forests. *Proceedings of the National Academy of Sciences of the United States of America*, *114*(31), 8307–8312. https://doi.org/10.1073/pnas.1706780114

Dubayah, R., Blair, J. B., Goetz, S., Fatoyinbo, L., Hansen, M., Healey, S., Hofton, M., Hurtt, G., Kellner, J., Luthcke, S., Armston, J., Tang, H., Duncanson, L., Hancock, S., Jantz, P., Marselis, S., Patterson, P. L., Qi, W., & Silva, C. (2020). The global ecosystem dynamics investigation: High-resolution laser ranging of the Earth's forests and topography. *Science of Remote Sensing*, *1*, 100002. https://doi.org/10.1016/j.srs.2020.100002

Duncanson, L., Rourke, O., & Dubayah, R. (2015). Small sample sizes yield biased allometric equations in temperate forests. *Scientific Reports*, *5*(1), 17153. https://doi.org/10.1038/srep17153

Ehbrecht, M., Schall, P., Ammer, C., & Seidel, D. (2017). Quantifying stand structural complexity and its relationship with forest management, tree species diversity and microclimate. *Agricultural and Forest Meteorology*, *242*, 1–9. https://doi.org/10.1016/j.agrformet.2017.04.012

Ehbrecht, M., Seidel, D., Annighöfer, P., Kreft, H., Köhler, M., Zemp, D. C., Puettmann, K., Nilus, R., Babweteera, F., Willim, K., Stiers, M., Soto, D., Boehmer, H. J., Fisichelli, N., Burnett, M., Juday, G., Stephens, S. L., & Ammer, C. (2021). Global patterns and climatic controls of forest structural complexity. *Nature Communications*, *12*(1), 519. https://doi.org/10.1038/s41467-020-20767-z

Ellsworth, D. S., & Reich, P. B. (1993). Canopy structure and vertical patterns of photosynthesis and related leaf traits in a deciduous forest. *Oecologia*, *96*(2), 169–178. https://doi.org/10.1007/BF00317729

Enquist, B. J., Norberg, J., Bonser, S. P., Violle, C., Webb, C. T., Henderson, A., Sloat, L. L., & Savage, V. M. (2015). Chapter Nine—Scaling from traits to ecosystems: Developing a general trait driver theory via integrating trait-based and metabolic scaling theories. In S. Pawar, G. Woodward, & A. I. Dell (Eds.), *Advances in ecological research* (Vol. 52, pp. 249–318). Academic Press. https://doi.org/10.1016/bs.aecr.2015.02.001

Enquist, B. J., West, G. B., & Brown, J. H. (2009). Extensions and evaluations of a general quantitative theory of forest structure and dynamics. *Proceedings of the National Academy of Sciences of the United States of America*, *106*(17), 7046–7051. https://doi.org/10.1073/pnas.0812303106

Fahey, R. T., Alveshere, B. C., Burton, J. I., D'Amato, A. W., Dickinson, Y. L., Keeton, W. S., Kern, C. C., Larson, A. J., Palik, B. J., Puettmann, K. J., Saunders, M. R., Webster, C. R., Atkins, J. W., Gough, C. M., & Hardiman, B. S. (2018). Shifting conceptions of complexity in forest management and silviculture. *Forest Ecology and Management*, *421*, 59–71. https://doi.org/10.1016/j.foreco.2018.01.011

Fahey, R. T., Atkins, J. W., Gough, C. M., Hardiman, B. S., Nave, L. E., Tallant, J. M., Nadehoffer, K. J., Vogel, C., Scheuermann, C. M., Stuart-Haëntjens, E., Haber, L. T., Fotis, A. T., Ricart, R., & Curtis, P. S. (2019). Defining a spectrum of integrative trait-based vegetation canopy structural types. *Ecology Letters*, *22*(12), 2049–2059. https://doi.org/10.1111/ele.13388

Fahey, R. T., Fotis, A. T., & Woods, K. D. (2015a). Quantifying canopy complexity and effects on productivity and resilience in late-successional hemlock–hardwood forests. *Ecological Applications*, *25*(3), 834–847. https://doi.org/10.1890/14-1012.1

Fahey, R. T., Fotis, A. T., & Woods, K. D. (2015b). Quantifying canopy complexity and effects on productivity and resilience in late-successional hemlock–hardwood forests. *Ecological Applications*, *25*(3), 834–847. https://doi.org/10.1890/14-1012.1

Farrior, C. E., Bohlman, S. A., Hubbell, S., & Pacala, S. W. (2016). Dominance of the suppressed: Power-law size structure in tropical forests. *Science*, *351*(6269), 155–157. https://doi.org/10.1126/science.aad0592

Ferguson, S. H., & Archibald, D. J. (2002). The 3/4 power law in forest management: How to grow dead trees. *Forest Ecology and Management*, *169*(3), 283–292. https://doi.org/10.1016/S0378-1127(01)00766-6

Fotis, A. T., & Curtis, P. S. (2017). Effects of structural complexity on within-canopy light environments and leaf traits in a northern mixed deciduous forest. *Tree Physiology*, *37*(10), 1426–1435. https://doi.org/10.1093/treephys/tpw124

Fotis, A. T., Murphy, S. J., Ricart, R. D., Krishnadas, M., Whitacre, J., Wenzel, J. W., Queenborough, S. A., & Comita, L. S. (2018). Above-ground biomass is driven by mass-ratio effects and stand structural attributes in a temperate deciduous forest. *Journal of Ecology*, *106*(2), 561–570. https://doi.org/10.1111/1365-2745.12847

Fox, J., Weisberg, S., Price, B., Adler, D., Bates, D., Baud-Bovy, G., Bolker, B., Ellison, S., Firth, D., Friendly, M., Gorjanc, G., Graves, S., Heiberger, R., Krivitsky, P., Laboissiere, R., Maechler, M., Monette, G., Murdoch, D., Nilsson, H., & R-Core. (2021). *car: Companion to applied regression* (3.0-11) [Computer software]. Retrieved from https://CRAN.R-project.org/package=car

Frenne, P. D., Zellweger, F., Rodríguez-Sánchez, F., Scheffers, B. R., Hylander, K., Luoto, M., Vellend, M., Verheyen, K., & Lenoir, J. (2019). Global buffering of temperatures under forest canopies. *Nature Ecology & Evolution*, *3*(5), 744. https://doi.org/10.1038/s41559-019-0842-1

Gough, C. M., Atkins, J. W., Fahey, R. T., Hardiman, B. S., & LaRue, E. A. (2020). Community and structural constraints on the complexity of eastern North American forests. *Global Ecology and Biogeography*, *29*(12), 2107–2118. https://doi.org/10.1111/geb.13180

Hallé, F., Oldeman, R. A. A., & Tomlinson, P. B. (1978). Opportunistic tree architecture. In F. Hallé, R. A. A. Oldeman, & P. B. Tomlinson (Eds.), *Tropical trees and forests: An architectural analysis* (pp. 269–331). Springer. https://doi.org/10.1007/978-3-642-81190-6_4

Hansen, M. C., Stehman, S. V., & Potapov, P. V. (2010). Quantification of global gross forest cover loss. *Proceedings of the National Academy of Sciences of the United States of America*, *107*(19), 8650–8655. https://doi.org/10.1073/pnas.0912668107

Hardiman, B. S., Gough, C. M., Halperin, A., Hofmeister, K. L., Nave, L. E., Bohrer, G., & Curtis, P. S. (2013). Maintaining high rates of carbon storage in old forests: A mechanism linking canopy structure to forest function. *Forest Ecology and Management*, *298*, 111–119. https://doi.org/10.1016/j.foreco.2013.02.031

Hardiman, B. S., LaRue, E. A., Atkins, J. W., Fahey, R. T., Wagner, F. W., & Gough, C. M. (2018). Spatial variation in canopy structure across forest landscapes. *Forests*, *9*(8), 474. https://doi.org/10.3390/f9080474

Horn, H. S. (1971). *The adaptive geometry of trees*. Princeton University Press.

Hulshof, C. M., & Spasojevic, M. J. (2020). The edaphic control of plant diversity. *Global Ecology and Biogeography*, *29*(10), 1634–1650. https://doi.org/10.1111/geb.13151

Ishii, H., & Asano, S. (2010). The role of crown architecture, leaf phenology and photosynthetic activity in promoting complementary use of light among coexisting species in temperate forests. *Ecological Research*, *25*(4), 715–722. https://doi.org/10.1007/s11284-009-0668-4

Ishii, H. T., Tanabe, S., & Hiura, T. (2004). Exploring the relationships among canopy structure, stand productivity, and biodiversity of temperate forest ecosystems. *Forest Science*, *50*(3), 342–355. https://doi.org/10.1093/forestscience/50.3.342

Kellner, J. R., Asner, G. P., Kinney, K. M., Loarie, S. R., Knapp, D. E., Kennedy-Bowdoin, T., Questad, E. J., Cordell, S., & Thaxton, J. M. (2011). Remote analysis of biological invasion and the impact of enemy release. *Ecological Applications*, *21*(6), 2094–2104. https://doi.org/10.1890/10-0859.1

Lagrue, C., Poulin, R., & Cohen, J. E. (2015). Parasitism alters three power laws of scaling in a metazoan community: Taylor's law, density-mass allometry, and variance-mass allometry. *Proceedings of the National Academy of Sciences of the United States of America*, *112*(6), 1791–1796. https://doi.org/10.1073/pnas.1422475112

Lefsky, M. A., Cohen, W. B., Parker, G. G., & Harding, D. J. (2002). Lidar Remote Sensing for Ecosystem Studies: Lidar, an emerging remote sensing technology that directly measures the three-dimensional distribution of plant canopies, can accurately estimate vegetation structural attributes and should be of particular interest to forest, landscape, and global ecologists. *BioScience*, *52*(1), 19–30. https://doi.org/10.1641/0006-3568(2002)052[0019:LRSFES]2.0.CO;2

MacArthur, R. H., & MacArthur, J. W. (1961). On bird species diversity. *Ecology*, *42*(3), 594–598. https://doi.org/10.2307/1932254

Marquet, P. A., Quiñones, R. A., Abades, S., Labra, F., Tognelli, M., Arim, M., & Rivadeneira, M. (2005). Scaling and power-laws in ecological systems. *Journal of Experimental Biology*, *208*(9), 1749–1769. https://doi.org/10.1242/jeb.01588

Martin-Ducup, O., Ploton, P., Barbier, N., Takoudjou, S. M., Mofack, G., Kamdem, N. G., Fourcaud, T., Sonké, B., Couteron, P., & Pélissier, R. (2020). Terrestrial laser scanning reveals convergence of tree architecture with increasingly dominant crown canopy position. *Functional Ecology*, *34*(12), 2442–2452. https://doi.org/10.1111/1365-2435.13678

McMahon, T. (1973). Size and shape in biology: Elastic criteria impose limits on biological proportions, and consequently on metabolic rates. *Science*, *179*(4079), 1201–1204. https://doi.org/10.1126/science.179.4079.1201

National Ecological Observatory Network (NEON). (2021). *Woody plant vegetation structure (DP1.10098.001): RELEASE-2021* (RELEASE-2021, p. 624.3 MB) [Csv]. National Ecological Observatory Network (NEON). https://doi.org/10.48443/E3QN-XW47

Parker, G. G., Harding, D. J., & Berger, M. L. (2004). A portable LIDAR system for rapid determination of forest canopy structure. *Journal of Applied Ecology*, *41*(4), 755–767. https://doi.org/10.1111/j.0021-8901.2004.00925.x

Parker, G. G., O'Neill, J. P., & Higman, D. (1989). Vertical profile and canopy organization in a mixed deciduous forest. *Vegetatio*, *85*(1), 1–11. https://doi.org/10.1007/BF00042250

R Core Team. (2020). *R: A language and environment for statistical computing*. (3.6.2) [Computer software]. Retrieved from http://www.R-project.org/

Saarinen, N., Calders, K., Kankare, V., Yrttimaa, T., Junttila, S., Luoma, V., Huuskonen, S., Hynynen, J., & Verbeeck, H. (2021). Understanding 3D structural complexity of individual Scots pine trees with different management history. *Ecology and Evolution*, *11*(6), 2561–2572. https://doi.org/10.1002/ece3.7216

Schraik, D., Hovi, A., & Rautiainen, M. (2021). Crown level clumping in Norway spruce from terrestrial laser scanning measurements. *Agricultural and Forest Meteorology*, *296*, 108238. https://doi.org/10.1016/j.agrformet.2020.108238

Seekell, D. A., Pace, M. L., Tranvik, L. J., & Verpoorter, C. (2013). A fractal-based approach to lake size-distributions. *Geophysical Research Letters*, *40*(3), 517–521. https://doi.org/10.1002/grl.50139

Smith, W. K., & Brewer, C. A. (1994). The adaptive importance of shoot and crown architecture in conifer trees. *The American Naturalist*, *143*(3), 528–532. https://doi.org/10.1086/285618

Sprugel, D. G. (1989). The relationship of evergreenness, crown architecture, and leaf size. *The American Naturalist*, *133*(4), 465–479. https://doi.org/10.1086/284930

Stark, S. C., Enquist, B. J., Saleska, S. R., Leitold, V., Schietti, J., Longo, M., Alves, L. F., Camargo, P. B., & Oliveira, R. C. (2015). Linking canopy leaf area and light environments with tree size distributions to explain Amazon forest demography. *Ecology Letters*, *18*(7), 636–645. https://doi.org/10.1111/ele.12440

Taubert, F., Fischer, R., Groeneveld, J., Lehmann, S., Müller, M. S., Rödig, E., Wiegand, T., & Huth, A. (2018). Global patterns of tropical forest fragmentation. *Nature*, *554*(7693), 519–522. https://doi.org/10.1038/nature25508

Taylor, L. R. (1961). Aggregation, variance and the mean. *Nature*, *189*(4766), 732–735. https://doi.org/10.1038/189732a0

Tippett, M. K., & Cohen, J. E. (2016). Tornado outbreak variability follows Taylor's power law of fluctuation scaling and increases dramatically with severity. *Nature Communications*, *7*(1), 10668. https://doi.org/10.1038/ncomms10668

Tomlinson, P. B. (1987). Architecture of tropical plants. *Annual Review of Ecology and Systematics*, *18*(1), 1–21. https://doi.org/10.1146/annurev.es.18.110187.000245

Verbeeck, H., Bauters, M., Jackson, T., Shenkin, A., Disney, M., & Calders, K. (2019). Time for a plant structural economics spectrum. *Frontiers in Forests and Global Change*, *2*, 43. https://doi.org/10.3389/ffgc.2019.00043

Wales, S. B., Kreider, M. R., Atkins, J., Hulshof, C. M., Fahey, R. T., Nave, L. E., Nadelhoffer, K. J., & Gough, C. M. (2020). Stand age, disturbance history and the temporal stability of forest production. *Forest Ecology and Management*, *460*, 117865. https://doi.org/10.1016/j.foreco.2020.117865

Walter, J. A., Fleck, R., Pace, M. L., & Wilkinson, G. M. (2020). Scaling relationships between lake surface area and catchment area. *Aquatic Sciences*, *82*(3), 47. https://doi.org/10.1007/s00027-020-00726-y

West, G. B., Brown, J. H., & Enquist, B. J. (1997). A general model for the origin of allometric scaling laws in biology. *Science*, *276*(5309), 122–126. https://doi.org/10.1126/science.276.5309.122

West, G. B., Brown, J. H., & Enquist, B. J. (1999). The fourth dimension of life: Fractal geometry and allometric scaling of organisms. *Science*, *284*(5420), 1677–1679. https://doi.org/10.1126/science.284.5420.1677

West, G. B., Enquist, B. J., & Brown, J. H. (2009). A general quantitative theory of forest structure and dynamics. *Proceedings of the National Academy of Sciences of the United States of America*, *106*(17), 7040–7045. https://doi.org/10.1073/pnas.0812294106

Wright, I. J., Reich, P. B., Westoby, M., Ackerly, D. D., Baruch, Z., Bongers, F., Cavender-Bares, J., Chapin, T., Cornelissen, J. H. C., Diemer, M., Flexas, J., Garnier, E., Groom, P. K., Gulias, J., Hikosaka, K., Lamont, B. B., Lee, T., Lee, W., Lusk, C., … Villar, R. (2004). The worldwide leaf economics spectrum. *Nature*, *428*(6985), 821–827. https://doi.org/10.1038/nature02403

Xu, M., Schuster, W. S. F., & Cohen, J. E. (2015). Robustness of Taylor's law under spatial hierarchical groupings of forest tree samples. *Population Ecology*, *57*(1), 93–103. https://doi.org/10.1007/s10144-014-0463-0

Xu, Y., Li, C., Sun, Z., Jiang, L., & Fang, J. (2019). Tree height explains stand volume of closed-canopy stands: Evidence from forest inventory data of China. *Forest Ecology and Management*, *438*, 51–56. https://doi.org/10.1016/j.foreco.2019.01.054

Zhao, L., Sheppard, L. W., Reid, P. C., Walter, J. A., & Reuman, D. C. (2019). Proximate determinants of Taylor's law slopes. *Journal of Animal Ecology*, *88*(3), 484–494. https://doi.org/10.1111/1365-2656.12931

SUPPORTING INFORMATION

Additional supporting information may be found in the online version of the article at the publisher's website.

How to cite this article: Atkins, J. W., Walter, J. A., Stovall, A. E. L., Fahey, R. T., & Gough, C. M. (2021). Power law scaling relationships link canopy structural complexity and height across forest types. *Functional Ecology*, 00, 1–14. https://doi.org/10.1111/1365-2435.13983